Electrochemistry Communications 12 (2010) 1432–1435

Contents lists available at ScienceDirect

Electrochemistry Communications

journal homepage: www.elsevier.com/locate/elecom

A quantum dot sensitized solar cell based on vertically aligned carbon nanotube templated ZnO arrays

J. Chen [a], C. Li [a,b], D.W. Zhao [c], W. Lei [a,*], Y. Zhang [b,*], M.T. Cole [b], D.P. Chu [b], B.P. Wang [a], Y.P. Cui [a], X.W. Sun [c], W.I. Milne [b,d]

[a] School of Electronic Science and Engineering, Southeast University, Nanjing 210096, China
[b] Electrical Engineering Division, Engineering Department, University of Cambridge, 9 JJ Thomson Avenue, CB3 0FA, Cambridge, UK
[c] School of Electrical and electronic Engineering, Nanyang Technological University, Nanyang Avenue, Singapore 639798, Singapore
[d] Department of Information Display, Kyung Hee University, Seoul 130-701, Republic of Korea

ARTICLE INFO

Article history:
Received 8 June 2010
Received in revised form 14 July 2010
Accepted 3 August 2010
Available online 10 August 2010

Keywords:
Quantum dot
Solar cell
VACNT
CdSe
ZnO

ABSTRACT

We report on a quantum dot sensitized solar cell (QDSSC) based on ZnO nanorod coated vertically aligned carbon nanotubes (VACNTs). Electrochemical impedance spectroscopy shows that the electron lifetime for the device based on VACNT/ZnO/CdSe is longer than that for a device based on ZnO/CdSe, indicating that the charge recombination at the interface is reduced by the presence of the VACNTs. Due to the increased surface area and longer electron lifetime, a power conversion efficiency of 1.46% is achieved for the VACNT/ZnO/CdSe devices under an illumination of one Sun (AM 1.5G, 100 mW/cm^2).

1. Introduction

Quantum dot sensitized solar cells (QDSSCs) have attracted extensive interest as a means of fabricating highly efficient, low cost photovoltaics [1]. QDs such as CdS [2–4], CdSe [5] and CdTe [6] demonstrate size-dependent band gaps which provide wide-ranging opportunities for harvesting light energy in the visible and infrared spectra. QDs are especially appealing for their high extinction coefficients compared to more conventional dyes. In addition, due to the impact ionization effect, it is possible to utilize hot electrons in QDs to generate multiple electron-hole pairs per photon [7]. Thus, the power conversion efficiency (PCE) of this variety of solar cell may indeed exceed the Shockley and Queisser limit (31%) [8].

Thus far, the efficiencies of QDSSCs are rather low. The major challenge of improving the performance of QDSSCs is to inhibit charge recombination at the semiconductor surface. One-dimensional (1D) semiconductors, such as TiO_2 nanotubes [6], ZnO nanowires [9], and Si nanowires [10], employed as direct electron pathways, have proven to provide an effective charge transport. Among these 1D nano-materials, carbon nanotubes (CNTs) have attracted much attention since they provide a large surface area, high electron mobility and chemical stability. In QDSSCs CNTs can be used as conducting scaffolds to capture and transport electrons from the QDs, or TiO_2 film, to the electrode surface [11,12]. Similarly, CNTs can be used as the counter electrode to reduce the charge transfer resistance along the counter electrode and electrolyte interface to enable long-term stability in QDSSCs [13].

In this paper, we report on the fabrication and characterization of QDSSCs based on ZnO nanorod coated vertically aligned carbon nanotube (VACNT) arrays. A PCE of 1.46% is obtained for our device using VACNTs/ZnO/CdSe as the photoanode.

2. Experimental details

Fluorine-doped tin dioxide (FTO)/quartz (Solaronix) slides (10 mm × 10 mm) were ultrasonically cleaned in de-ionized water, acetone, and iso-propanol alcohol, and were dried at 100 °C in an atmospheric pressure oven. VACNT arrays were grown by Plasma Enhanced Chemical Vapour Deposition (PE-CVD) at 500 °C using a magnetron sputtered, 7 nm-thick Ni catalyst with photolithographically defined 6 μm spacing. The VACNT fabrication process is described in detail in previous work [14]. ZnO nanorods were simultaneously synthesized and deposited on the surface of the VACNTs by a hydrothermal method. A ZnO seed layer was deposited on the VACNT arrays and FTO glass by ultrasonic spray pyrolysis for 5 min, respectively. The substrates were then immersed into a 0.01 M zinc nitrate and 0.01 M hexamethylenetetramine solution in an autoclavable screw cap bottle and heated at 95 °C for 10 h. Pre-synthesized thioglycolic acid capped-CdSe QDs, with a diameter of 4.5 nm, were then loaded onto the ZnO nanorod surface [15]. A ZnO/CdSe

* Corresponding authors. Tel.: +86 25 83792449; fax: +86 25 833632222.
E-mail addresses: lw@seu.edu.cn (W. Lei), yz236@cam.ac.uk (Y. Zhang).

1388-2481/$ – see front matter © 2010 Elsevier B.V. All rights reserved.
doi:10.1016/j.elecom.2010.08.001

photoanode was fabricated for comparison. Finally, Pt was sputtered on ITO as the counter electrode, a thermal-plastic spacer applied, and an electrolyte solution of polysulfide consisting of 2 M Na_2S and 3 M S was introduced. Herein, QDSSCs consisting of ZnO/CdSe and VACNT/ZnO/CdSe are defined as cells A and B, respectively.

VACNT arrays were synthesized using a commercially available PE-CVD system (AIXTRON-Black Magic). Current density–voltage (*J*–*V*) characteristics were measured with a Keithley 2440 Sourcemeter under 100 mW/cm^2 (AM 1.5G) illumination from a solar simulator (Abet-technologies, U.S.A.). Electrochemical impedance spectra (EIS) were measured under open-circuit voltage with an oscillation voltage amplitude of 10 mV for frequencies from 10^{-1} to 10^6 Hz. The obtained impedance spectra were fitted using Z-view software.

3. Results and discussion

Fig. 1(a) shows the absorption spectra of ZnO/CdSe and VACNT/ZnO/CdSe photoanodes which exhibit a characteristic sharp peak at their band edges. The inset of Fig. 1(a) shows a TEM image of CdSe QDs with a diameter of 4–5 nm uniformly dispersing in the ethanol solution. Fig. 1(b) shows a SEM image of VACNTs grown in a hexagonal array. Fig. 1(c) shows the SEM image of ZnO nanorods vertically grown on FTO substrate with a length of 2 μm. Fig. 1(d) shows the cross-sectional SEM image of a VACNT array coated with ZnO nanorods before sensitizing with CdSe QDs. It is obvious that the CNTs, which function as the templates for the ZnO nucleation, are perpendicular to the substrate and have a length of 5 μm. We note that

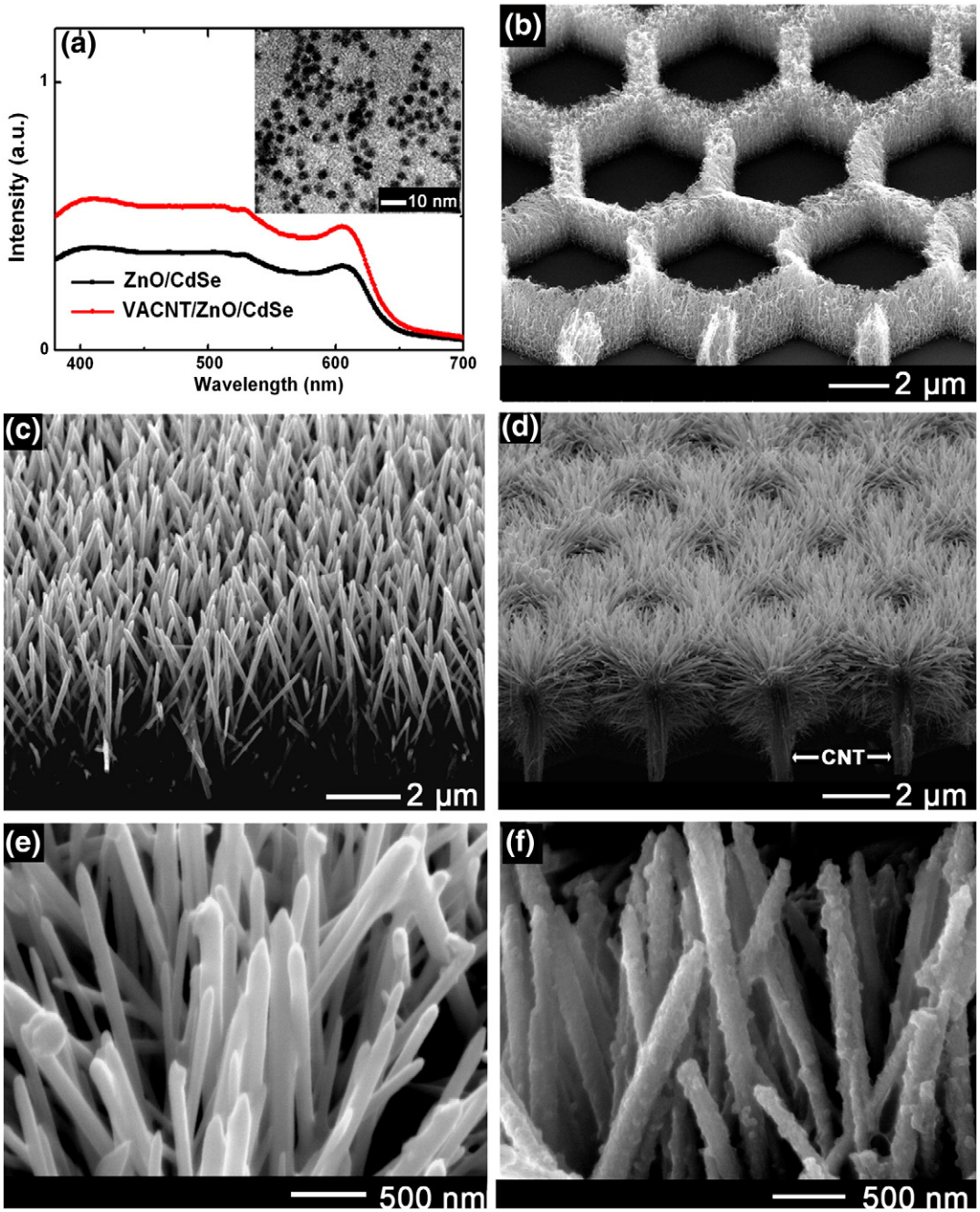

Fig. 1. (a) The absorption spectra of ZnO/CdSe and VACNT/ZnO/CdSe photoanodes. The inset is the TEM image of QDs. SEM image of (b) VACNT. (c) ZnO. (d) VACNT/ZnO. (e) VACNT/ZnO before sensitizing with CdSe QD. (f) VACNT/ZnO after sensitizing with CdSe QD.

ZnO nanorods, with a length of 2 μm and a diameter of 60 nm, fully cover the VACNT surface, and therefore largely increase the number of sites for QD adsorption. It is also worth noting that the use of VACNTs results in an increased spectral transmission due to their 1D nanostructure, ensuring increased light absorption in the photoactive layer [16]. In our cells, we also observe this low loss characteristic enhanced by the effective linearity of the VACNT scaffolds, giving significant spectral transmission through the hexagonal channel directly to the photo-active QD sites.

Fig. 1(e) and (f) shows the SEM images of VACNT arrays coated with ZnO nanorods before and after sensitizing with CdSe QDs. Here it is evident that the surface of the VACNT/ZnO nanorods becomes rougher following QD dispersion. The concentration of QDs adsorbed onto the photoanodes can be calculated by the concentration difference of the QD solutions before and after sensitization: 5.4×10^{-7} M and 2.8×10^{-6} M for ZnO and CNT/ZnO, respectively. The increased amount of QDs assembled on ZnO based device is primarily due to the enlarged surface area in the engineered VACNT/ZnO nanostructure.

Fig. 2(a) shows an energy level schematic diagram for VACNT, ZnO and CdSe QD. From the excitonic transition wavelength of 605 nm for the CdSe QDs as shown in Fig. 1(a), the size of the QDs is estimated to be 4.5 nm with a band gap of around 1.99 eV [17]. The work function of a typical CNT is 4.5–5.0 eV [16]. From the schematic it can be observed that the conduction bands of the CdSe and ZnO and the work function of VACNT form an energy step for the electron transport, thereby facilitating electron transfer. Fig. 2(b) shows *I–V* characteristics under 100 mW/cm^2 illumination for VACNT/ZnO with length of ZnO varying from 0.5 to 2.5 μm. It can be seen that the short-circuit current density (J_{sc}) increases as the length of ZnO increases (from 0.5 to 2 μm), which implies that the amount of CdSe QDs adsorbed on ZnO increases. The maximum PCE value of QDSSC is 1.46% with $J_{sc}=4.45$ mA/cm^2, $V_{oc}=0.57$ V, and FF = 57.5% for 2 μm length of ZnO. However, when the length of ZnO increases to 2.5 μm, the PCE of cell reduces, due to the decrease of photocurrent density and FF. It is possibly that the longer ZnO nanorods cover the hexagonal channels which can be largely reduced the spectral transmission. Fig. 2(c) shows the *I–V* characteristics for cells A and B under 100 mW/cm^2 illumination and in dark. Cell A has a PCE of 0.88% with short-circuit current density (J_{sc}) of 3.86 mA/cm^2, open-circuit voltage (V_{oc}) of 0.547 V, and fill factor (FF) of 42.7%. With the incorporation of VACNT arrays (cell B) the QDSSC leads to an improved PCE. The J_{sc} for cell B is increased slightly, most likely due to the increased QD adsorption. The FF for cell B is higher than that for cell A, demonstrating that the charge recombination is inhibited by the presence of the VACNT arrays. In addition, the energy barrier at VACNT/ZnO interface can be effective in suppressing the interfacial recombination, leading to the increased values of V_{oc} and FF [16]. Fig. 2(d) shows the photovoltaic response to repeated on–off cycles of visible irradiation. Compared to cell A, cell B exhibits stable photovoltage generation during the irradiation on–off cycle.

In order to reveal the interfacial reactions of photoexcited electrons in our QDSSCs, EIS of the as-prepared QDSSC were measured. Fig. 3(a) shows typical Nyquist plots of the QDSSCs (cells A and B). Two semi-circles exist in the high-frequency region and middle-frequency region for both cells. The electron lifetime (τ_r) in the oxide film can be estimated by $\tau_r=1/2\pi f_{max}$, where f_{max} is the maximum frequency of the middle-frequency peak [18]. As indicated in circles of Fig. 3(b), the f_{max} value for cell B is 6.1 Hz, smaller than that for cell A (18.3 Hz). Correspondingly, the electron lifetime is calculated to be 8.7 and 26.1 ms for cells A and B, respectively. The longer electron lifetime for cell B implies that the back reaction for

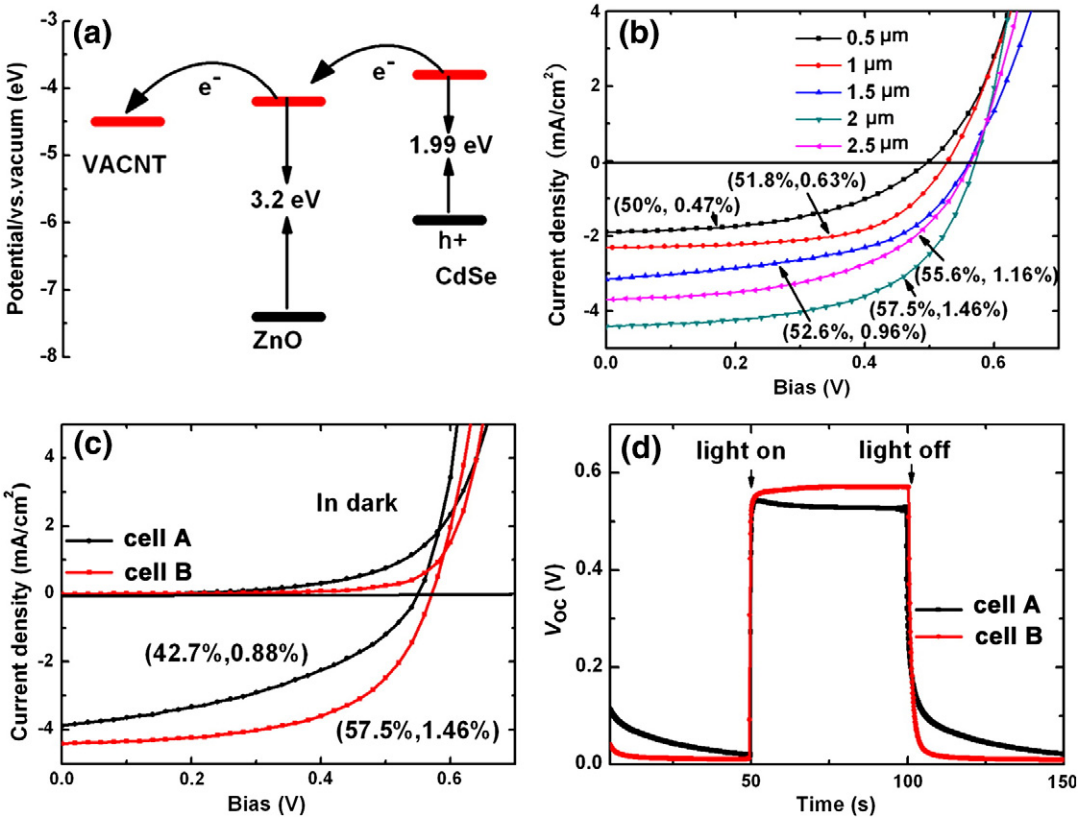

Fig. 2. (a) The energy schematic diagram for VACNT, ZnO and CdSe QD. (b) *I–V* characteristics of VACNT/ZnO/CdSe cells with length of ZnO varying from 0.5 to 2.5 μm at 100 mW/cm^2 illumination. (c) *I–V* characteristics of ZnO/CdSe and VACNT/ZnO/CdSe cells at 100 mW/cm^2 illumination. (d) Photovoltaic response during illumination on–off cycle.

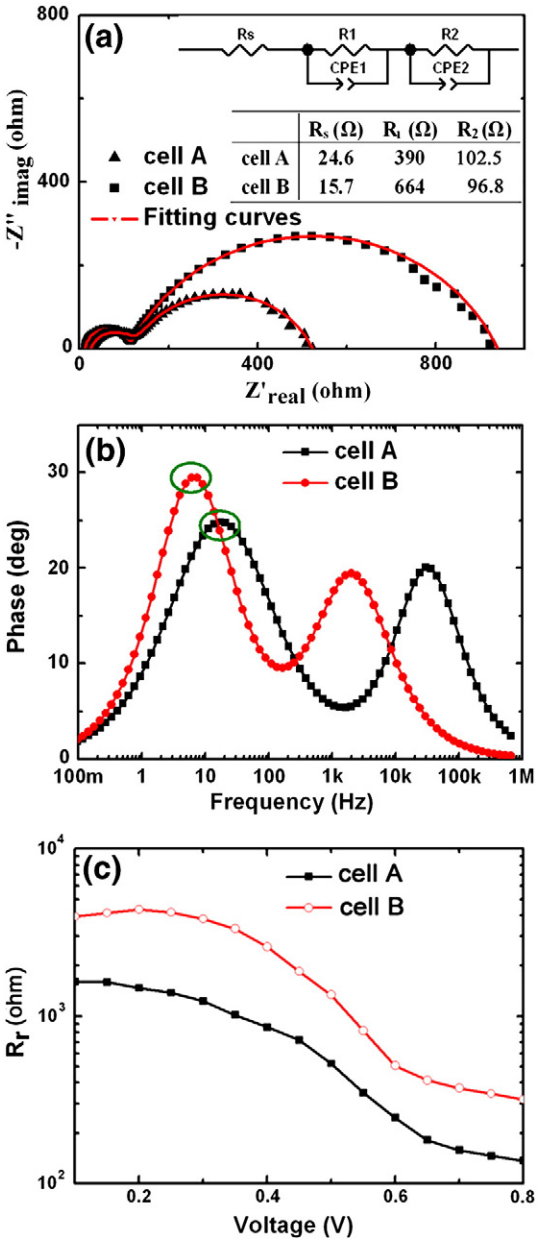

	R_s (Ω)	R_1 (Ω)	R_2 (Ω)
cell A	24.6	390	102.5
cell B	15.7	664	96.8

Fig. 3. (a) Nyquist plots of the fabricated QDSSCs. The insets are the equivalent circuit and values of fitting parameters. R_1 is the recombination resistance R_r. (b) Bode phase plots. (c) R_r at various applied voltages for ZnO/CdSe and VACNT/ZnO/CdSe electrodes.

electrons between the conduction band of ZnO and the electrolyte is effectively suppressed [19], leading to a higher FF and improved PCE. Fig. 3(c) shows the recombination resistance (R_r) at various applied voltages for both cells. The middle-frequency semi-circle is correlated with the chemical capacitance and recombination resistance (R_r). Using the equivalent circuit as shown in the inset of Fig. 3(a), the R_r at various applied voltages can be measured. It is clear that the R_r value decreases with an increase in voltage for both cells. However, the value of R_r for cell B is higher than that for cell A, demonstrating that the charge recombination is efficiently suppressed due to the presence of the VACNT arrays.

4. Conclusion

We have fabricated a QDSSC based on VACNT arrays coated with ZnO nanorods. The improved performance of the VACNT/ZnO/CdSe photoanode is mainly due to the increased J_{sc} and FF. The enlarged surface area for VACNTs coated with ZnO nanorods provides more sites for CdSe QD loading, leading to a higher J_{sc}. A longer electron lifetime for VACNT/ZnO/CdSe also demonstrates that VACNT arrays indeed play a beneficial role in facilitating charge transport and the suppression of interfacial charge recombination, leading to an increased FF. As a result, a PCE of 1.46% is achieved for our VACNT/ZnO/CdSe device, amounting to a 40% improvement on ZnO/CdSe devices.

Acknowledgement

The authors gratefully thank the financial supports by National Science Foundation of China (No.: 50872022, 60801002, 60971017), National Key Basic Research Program 97 (2010CB327705), the Chinese 111 project (B07027), the “863” Program of China (2007AA01Z303, 2008AA03A314), NSF Project of Jiangsu province (BK2008319, BK2009264), Scientific Research Foundation of Graduate School of Southeast University YBJJ1002.

References

[1] D.R. Baker, P.V. Kamat, Adv. Func. Mater. 19 (2009) 805.
[2] Q.X. Zhang, Y.D. Zhang, S.Q. Huang, X.M. Huang, Y.H. Luo, Q.B. Meng, D.M. Li, Electrochem. Commun. 12 (2010) 327.
[3] C.H. Chang, Y.L. Lee, Appl. Phys. Lett. 91 (2007) 053503.
[4] W. Lee, S.K. Min, V. Dhas, S.B. Ogale, S.H. Han, Electrochem. Commun. 11 (2009) 103.
[5] J. Chen, J.L. Song, X.W. Sun, W.Q. Deng, C.Y. Jiang, W. Lei, J.H. Huang, R.S. Liu, Appl. Phys. Lett. 94 (2009) 153115.
[6] X.F. Gao, H.B. Li, W.T. Sun, Q. Chen, F.Q. Tang, L.M. Peng, J. Phys. Chem. C 113 (2009) 7531.
[7] A.J. Nozik, Inorg. Chem. 44 (2005) 6893.
[8] W. Shockley, H.J. Queisser, J. Appl. Phys. 32 (1961) 510.
[9] Y. Zhang, T.F. Xie, T.F. Jiang, X. Wei, S. Pang, X. Wang, D. Wang, Nanotechnology 20 (2009) 155707.
[10] B.Z. Tian, X.L. Zheng, T.J. Kempa, Y. Fang, N.F. Yu, G.H. Yu, J.L. Huang, C.M. Lieber, Nature 449 (2007) 885.
[11] B. Farrow, P.V. Kamat, J. Am. Chem. Soc. 131 (2009) 11124.
[12] A. Kongkanand, R.M. Dominguez, P.V. Kamat, Nano Lett. 7 (2007) 676.
[13] W.J. Lee, E. Ramasamy, D.Y. Lee, J.S. Song, Appl. Mater. Inter. 1 (2009) 1145.
[14] C. Li, Y. Zhang, M. Mann, P. Hiralal, H.E. Unalan, W. Lei, B. Wang, D. Chu, D. Pribat, G.A.J. Amaratunga, W.I. Milne, Appl. Phys. Lett. 96 (2010) 143114.
[15] X.W. Sun, J. Chen, J.L. Song, D.W. Zhao, W.Q. Deng, W. Lei, Opt. Exp. 18 (2010) 1296.
[16] J.W. Liu, Y.T. Kuo, K.J. Klabunde, C. Rochford, J. Wu, J. Li, Appl. Mater. Inter. 1 (2009) 1645.
[17] I. Robel, M. Kuno, P.V. Kamat, J. Am. Chem. Soc. 129 (2007) 4136.
[18] R. Kern, R. Sastrawan, J. Ferber, R. Stangl, J. Luther, Electrochim. Acta 47 (2002) 4213.
[19] W. Zhang, R. Zhu, X.Z. Liu, B. Liu, S. Ramakrishna, Appl. Phys. Lett. 95 (2009) 043304.